HHS Public Access

Author manuscript

Biomaterials. Author manuscript; available in PMC 2020 January 01.

Published in final edited form as:

Biomaterials. 2019 January ; 188: 130–143. doi:10.1016/j.biomaterials.2018.10.015.

Untangling the response of bone tumor cells and bone forming cells to matrix stiffness and adhesion ligand density by means of hydrogels

Tongmeng Jiang[#1,2,3], **Jinmin Zhao**[#1,2,3], **Shan Yu**[#4], **Zhengwei Mao**[4,*], **Changyou Gao**[4], **Ye Zhu**[5], **Chuanbin Mao**[5,6,*], and **Li Zheng**[1,2,3,*]

[1]Guangxi Engineering Center in Biomedical Materials for Tissue and Organ Regeneration & Guangxi Collaborative Innovation Center for Biomedicine, Life Sciences Institute, Guangxi Medical University, Nanning 530021, China

[2]Department of Orthopaedics Trauma and Hand Surgery, The First Affiliated Hospital of Guangxi Medical University, Nanning 530021, China

[3]Guangxi Key Laboratory of Regenerative Medicine, International Joint Laboratory on Regeneration of Bone and Soft Tissue, The First Affiliated Hospital of Guangxi Medical University, Nanning 530021, China

[4]MOE Key Laboratory of Macromolecular Synthesis and Functionalization, Department of Polymer Science and Engineering, Zhejiang University, 38# Zheda Road, Hangzhou 310027, China

[5]Department of Chemistry & Biochemistry, Stephenson Life Sciences Research Center, University of Oklahoma, 101 Stephenson Parkway, Norman, OK 73019-5300, USA

[6]School of Materials Science and Engineering, Zhejiang University, Hangzhou 310027, China

[#] These authors contributed equally to this work.

Abstract

How cancer cells and their anchorage-dependent normal counterparts respond to the adhesion ligand density and stiffness of the same extracellular matrix (ECM) is still not very clear. Here we investigated the effects of ECM adhesion ligand density and stiffness on bone tumor cells (osteosarcoma cells) and bone forming cells (osteoblasts) by using poly (ethylene glycol) diacrylate (PEGDA) and methacrylated gelatin (GelMA) hydrogels. By independently changing the PEGDA and GelMA content in the hydrogels, we achieved crosslinked hydrogel matrix with

[*]Co-Corresponding authors. zwmao@zju.edu.cn (Prof. Z. W. Mao), cbmao@ou.edu (Prof. C. B. Mao), zhengli224@163.com (Prof. L. Zheng).

Conflict of interests

The authors declare no conflict of interests.

Data Availability

All of the data reported in this work are available upon request.

independently tunable stiffness (1.6, 6 and 25 kPa for 5%, 10%, 15% PEDGA, respectively) and adhesion ligand density (low, medium and high for 0.05%, 0.2%, 0.5% GelMA respectively). By using a series of biochemical and cell biological characterizations as well as *in vivo* studies, we confirmed that osteosarcoma and osteoblastic cells responded differently to the stiffness and adhesion ligand density within 3D ECM. When cultured within the 3D PEGDA/GelMA hydrogel matrix, osteosarcoma cells are highly dependent on the matrix stiffness via regulating the integrin-mediated focal adhesion (FA) pathway, whereas osteoblasts are highly sensitive to the matrix adhesion ligand density through regulating the integrin-mediated adherens junction (AJ) pathway. However, when seeded on the 2D surface of the hydrogels, osteosarcoma cells behaved differently and became sensitive to the matrix adhesion ligand density because they were “forced” to attach to the substrate, similar to anchorage-dependent osteoblasts. This study might provide new insights into rational design of scaffolds for generating in vitro tumor models to test anticancer therapeutics and for regenerating tissue to repair defects.

Keywords

extracellular matrix; adhesion; stiffness; osteosarcoma; osteoblasts

1. Introduction

In most normal tissues, the extracellular matrix (ECM) adhesion ligands and stiffness play important roles in controlling cell fates. When cells are attached to a substrate, they first bind to cell adhesion ligands on the ECM through integrin receptors, which elicits a cascade of signals, such as adherens junction (AJ) signaling [1, 2], to connect the cytoskeleton and the ECM [3, 4]. In addition, cells can sense the ECM by pulling against it and to generate signals through mechano-transducers [5]. However, cell-ECM interactions are altered when malignant transformation occurs, such as in the case of invasion, uncontrollable cell proliferation, and unapicobasal polarity [6].

Unlike normal cells that depend on the contact with matrix, cancer cells always preserve cell death or growth in the absence of ECM adhesivity. Most oncogenic transformed cells are anchorage-independent and do not require attachment [7], leading to activation of the focal adhesion (FA) signaling pathway [8, 9] and a gradual loss in AJ protein expression. Badriprasad et al. reported that RGD-based integrin ligands had no effect on the cancer cell growth [10] but still impacted cancer cell metabolism and gene expression [11, 12]. Thus, adhesion ligands are not always required for cancer cell growth in a three dimensional (3D) matrix.

Accumulating evidence has shown that ECM rigidity is correlated with tumor stress and metastasis[13] and modulates tumor cell behavior through the regulation of local microenvironment[14]. Increasing ECM stiffness induces malignant phenotypes independently from the ligand density[15]. Cells sense matrix elasticity and transduce the information into morphological and functional changes, using cytoskeletal motors to create tension in actin structures that are associated with FAs and provide a force transmission pathway from inside the cell to the elastic matrix. Integrins on the cell surface are considered

mechanosensory receptors[16], and are important downstream molecules in the FA signaling pathway that act as mechano-transducers. Talin, paxillin and vinculin have been implicated in cytoplasmic adaption through the integrin binding domain/actin-binding region of these proteins[17, 18]. Focal adhesion kinase (FAK), an integral FA component that acts as a scaffolding protein, has been reported to be related to stimulation of tumor angiogenesis[19].

We hypothesized that when cells are shifted from a normal to a cancerous state, they might respond differently to the substrate. Matrix properties, primarily the adhesion capacity and rigidity, may elicit different cell responses when normal cells became cancerous. Therefore, it would be of interest to tune the mechanical strength and adhesivity separately in one material system to study their influence on the cell behaviors. Owing to their hydrophilic and bio-inert properties, polyethylene glycol diacrylate (PEGDA) gels are widely used as a model system to change hydrogel crosslinking density and subsequent material stiffness, without altering ligand/receptor density and the bioactivity of the hydrogels. Gels incorporating another bioactive component, such as methacrylated gelatin (GelMA), which has an RGD motif in its sequence and the ability to bind cells, exhibit advantages over non-adherent materials by modulating cell functions in anchorage-dependent cells, in part simply because of increased cell attachment[20]. Varying the ratio of PEGDA and GelMA in PEGDA/GelMA compound hydrogels permits manipulation of the matrix ligand density and stiffness separately and precisely without changing other properties[21]. In this study, the effects of ECM adhesion ligand density and stiffness on osteosarcoma cells and their normal counterparts (osteoblasts) were investigated using PEGDA and GelMA hydrogels with self-governed regulation of mechanical strength and adhesion ligand density (Fig. 1). The underlying mechanisms of the cell responses were also explored. This study might provide new insights for the rational design of scaffolds for tumor and tissue engineering.

2. Materials and methods

2.1 Synthesis of methacrylated gelatin (GelMA)

Briefly, 4 g of gelatin was dissolved in phosphate buffer (40 mL, pH=8.0) at 70°C. The gelatin solution was cooled to 45°C, and then 40 μL of methacrylic anhydride was slowly dropped in the solution with continuous stirring for 1 h. The reaction was terminated by the addition of another 40 mL of phosphate buffer (pH=8.0). The GelMA was precipitated in 500 mL of cold ethanol and obtained by centrifugation. The GelMA was dissolved in water and placed in a dialysis tube. A molecular weight cut-off (3500 Da) was obtained. After dialysis at 37°C for 5 days, the purified GelMA was lyophilized and stored at −20°C.

2.2 Fabrication of PEGDA-GelMA hydrogels

GelMA and Irgacure 2959 (BASF, Germany) were dissolved in phosphate-buffered saline (PBS) (0.1 M) at a final concentration of 0.5% (w/v) and 1% (w/v), respectively. Poly(ethylene glycol) diacrylate (PEGDA) monomers, GelMA and Irgacure 2959 were mixed in a 24-well plate with fixed ratios (Table 1) to obtain hydrogels with a range of ECM stiffness and adhesion ligand densities (Fig. 1). Gelation was carried out under a UV floodlight (80 mW/cm^2, Intelli-ray 400, Uvitron International, USA) for 10 min. Then hybrid hydrogels were washed in PBS to eliminate the excessive monomers and initiator.

2.3 Characterization of scaffolds

The GelMA and as-prepared hydrogels were characterized by ^{1}H NMR at 40°C with D_2O as a solvent. The equilibrium swelling ratios (ESR) of the hydrogels were studied. In brief, after the hydrogels were prepared and rinsed in PBS for 24 h, the mass of swollen hydrogel was recorded as W_{wet}. After being washed with plenty of water, the hydrogel was freeze-dried, and its mass was recorded as W_{dry}. The equilibrium swelling ratio was calculated according to the formula ESR = $(W_{wet}-W_{dry})/W_{dry}$. The hydrogels were shaped into cylinders (Φ =15mm, H= 3mm) and then tested using a mechanical tester at room temperature in a wet state. Then the compressive modulus was evaluated from the linear region (1.5–2.5% strain) with the compression rate at 2 mm/min. The hydrogels were freeze-dried and ripped into several pieces with tweezers. The surface and inter-section morphology of the hydrogels were observed with SEM.

2.4 Cell culture

Human osteosarcoma MG63 cells (cell bank of Shanghai Institutes for Biological Sciences, Shanghai, China) were cultured in culture media containing Roswell Park Memorial Institute (RPMI) 1640 medium (Thermo fisher, Shanghai, China), 1% penicillin/streptomycin (Solabio, Peking, China) and 10% fetal bovine serum (FBS, Zhejiang Tianhang Biotechnology Ltd, Hangzhou, China) at 37°C and 5% CO_2. The osteoblastic hFOB1.19 cells (cell bank of Shanghai Institutes for Biological Sciences, Shanghai, China) were cultured in culture media containing Dulbecco's Modified Eagle Medium: Nutrient Mixture F-12 (DMEM/F-12, Thermo fisher, Shanghai, China) with 0.3 mg/mL G418 (Gibco, Carlsbad, CA, USA) and 10% FBS at 34°C and 5% CO_2. All cells used in this study were in the logarithmic growth phase.

2.5 Cell adhesion assay

Cell attachment was measured by counting the living cells on the scaffold surface (LIVE/DEAD® Viability Kit, Invitrogen, Shanghai, China) after 24 h of culture. Briefly, osteoblastic hFOB1.19 cells were seeded on the surfaces of the nine PEGDA/GelMA hydrogels (10^4 cells/cm^2). 24 h later, the samples were stained using propidium iodide (PI, 4 μM) and calcein-AM (2 μM) and then observed using fluorescence microscopy (Olympus BX53, Japan). Cell adhesion areas were automatically counted per view (original magnification 200×, n=10) using ImageJ software (Release 1.5 h, Bethesda, MD, USA)[22, 23].

2.6 Cell seeding

Cells were encapsulated in the hydrogels or seeded on the surface, as shown in Fig. 1. Briefly, osteosarcoma and osteoblastic cells were dissociated by 0.25% trypsin (Solarbio, Beijing, China) and then centrifuged. For intrascaffold culture, cell pellets were vortexed with PEGDA-GelMA solution prior to gelation (10^6 cells/mL). Cell-gel composites were allowed to gel for 10 min under a UV floodlight (80 mW/cm^2, Intelli-ray 400) before 4 mL of standard culture medium was added. For FAK inhibition studies, intrascaffold-cultured osteosarcoma cells were treated with 10 μM PF-573228 (MedChem Express, NJ, USA). For

E-cadherin inhibition studies, intrascaffold-cultured osteoblasts were treated with 5 μg/ml anti-E–cadherin (SHE78–7, Zymed laboratories Inc., San Francisco, CA, USA).

For surface culture, cells were seeded on the surface of 9 scaffolds (1×10^5 cells/cm^2) that were flattened onto 6-well plates and allowed to gelate for 10 min under a UV floodlight in advance. MG63-gel composites were cultured at 5% CO_2 and 37°C, osteoblast-gel composites at 34°C and 5% CO_2.

2.7 MTT assay

Cell proliferation was quantified on day 3 and 7 by MTT (3-(4,5-dimethyl-2-thiazolyl)-2,5-diphenyl-2-H-tetrazolium bromide, 5 mg/mL). For intrascaffold-cultured cells, 100 μL of cell-gel composites were incubated in 1 mL of culture medium with 200 μL of MTT. Then, supernatants were discarded and the cell-gel composites were cool pulverized using a tissuelyser (Shanghai Jinxin Industrial Development Co. Ltd., Shanghai, China). For cells cultured on the gel surfaces, 1 mL of cultured media containing 200 μL of MTT were dropped into each well (6-well plate). After 4 h of incubation at 37°C, MTT formazan crystals were dissolved by 1 mL of Dimethyl sulfoxide (DMSO, Solarbio, Beijing, China). Then absorbance was evaluated with a microplate reader (Thermo, Shanghai, China) at 490 nm.

2.8 Cell viability assay

The viability of cells was investigated on day 7 using a LIVE/DEAD® Viability Kit (Invitrogen, Shanghai, China), which utilizes PI (4 μM) and calcein-AM (2 μM) to identify living and dead cells, respectively. All images were taken by a confocal microscope (Nikon A1, Tokyo, Japan).

2.9 Real-time qPCR

Total RNA of cell-scaffold composites was extracted after the composites were cultured for 7 days via a Total RNA-isolation kit (Magen, China) and quantified with a spectrophotometer (NanoDrop 2000, Shanghai, China). After the cDNA was synthesized, quantitative real-time PCR was carried out using Lightcycler® 96 kit (Roche, Switzerland). *GAPDH* was used as an internal control. The primer sequences targeting tumorigenesis-related genes (vascular endothelial growth factor (*VEGF*), matrix metallopeptidase 2 (*MMP2*), hypoxia inducible factor 1 alpha subunit (*HIFA*) and matrix metallopeptidase 9 (*MMP9*)) and osteogenesis-associated genes (runt-related transcription factor 2 (*RUNX 2*), bone morphogenetic protein 2 (*BMP 2*), collagen type I (*COL1*) and alkaline phosphatase (*ALP*)) are listed in Table S1.

2.10 Western blotting

All proteins were obtained from cell-scaffold composites after 7 days of culture using RIPA Lysis and Extraction Buffer (Beyotime, Peking, China) then detected using a BCA Kit (Beyotime, Peking, China) following standard western blot protocols. GAPDH (Glyceraldehyde-3-phosphate dehydrogenase) antibody was purchased from USCN Life Science (Wu Han, China). Adherens Junction Antibody Sample Kit and FAK Antibody Sample Kit were purchased from CST (Cell Signaling Technology, MA, USA). HIFA and

VEGF were purchased from Abcam (Beijing, China). MMP2, MMP9, ALP, COL1, BMP2 and RUNX2 were purchased from Boster Biological Technology (Wuhan, China). All samples were detected using goat anti-rabbit IgG Alexa Fluor® 790 infrared dye-conjugated secondary antibodies (Invitrogen, USA) and then scanned via an Odyssey Imaging System (LI-COR). The expression of proteins was calculated using ImageJ software.

2.11 Immunofluorescence staining

After cultured for 7 days *in vitro*, all intra-cultured cells were sliced into to 5-μm sections after being buried in paraffin. Mouse anti-human osteocalcin (OCN), ALP, MMP2, MMP9 and CD133 antibodies (Boster Biological Technology, Wuhan, China) at 1:200 dilutions were loaded in the sections at 4□ for 24h. Then samples were incubated using secondary antibodies (Boster, Wuhan, China). Fluorescence images were taken and analyzed using a microscope (Olympus BX53, Tokyo, Japan).

2.12 Aldehyde dehydrogenase (ALDH) activity

The activity of ALDH that is a marker for the malignancy of osteosarcoma [24] was tested. Briefly, after intrascaffold cultured for 7 days, the cell-gel composites of osteosarcoma were first placed on ice then ALDH was detected by an ALDH test kit (Solarbio, Beijing, China) as indicated by the manufacturer. All ALDH activities were evaluated using a microplate reader (Thermo, Peking, China) at 340 nm by measuring the production of NAD+[25].

2.13 Alkaline phosphatase (ALP) activity

The assay of the activity of ALP, a marker for osteoblast differentiation [26], was performed to evaluate the osteoblasts embedded in the scaffolds after 7 days of culture using an ALP kit (Nanjing Jiancheng Bioengineering Research Institute, Nanjing, China) as instructed.

2.14 Alizarin red staining

After 7 days of culture, sections of intrascaffold osteoblasts were stained using alizarin red (0.2%, Solarbio, Beijing, China) to evaluate the mineralization and ossification at room temperature for 30 min. Images were taken and analyzed by a microscope (Olympus BX53, Japan).

2.15 Animal studies

Animal studies were approved by the Animal Care and Welfare Committee of Guangxi Medical University. Athymic nude mice (4–5 weeks old) were anesthetized with a solution of ketamine and xylazine prior to the subcutaneous implantation of hydrogels containing MG63 cells or hFOB1.19 cells into their back. Cells were mixed with PEGDA/GelMA scaffolds at a concentration of 10^7 cells/100 μL scaffold and photocrosslinked prior to the subcutaneous implantation into the back of the anesthetized mice. Surgical incisions were sutured using 6–0 absorbable surgical sutures (Hwato, Suzhou, China). The neoplasms were measured using calipers, and the volume was calculated using the formula for the volume of an ellipsoid (volume=length×width×height×π). Three weeks after implantation, the mice were sacrificed by CO_2 inhalation, and all samples were harvested for microscopic observation and then for histological and immunohistochemical evaluation.

2.16 Statistical analysis

All data were measured by one-way ANOVA and Tukey's test via SPSS 16.0 software (IBM, USA), performed using the means ± standard deviation via Prism 5.0 (GraphPad, USA). Significant differences were set *at p*-values under 0.05.

3. Results

3.1 Tunable stiffness was obtained by varying the PEGDA content in PEGDA/GelMA hydrogels

GelMA was achieved by grafting polymerizable carbon double bonds to gelatin molecules through the reaction with MA in alkaline environment. Differed from the 1H NMR spectrum of gelatin, GelMA presented new resonance peaks at 5.60 and 5.36 ppm due to the presence of the protons in $H_2C=C(CH_3)$-. This confirmed the successful MA grafting (Fig. S1). For MA, the degree of substitution (DS) was tested to be 21.2% based on ^{1}H NMR spectroscopy[27]. By using Irgacure 2959 as the initiator, the hydrogels were formed within 10 min at room temperature. We did not observe the carbon double bond signal after gelation, indicating the complete polymerization.

The compressive modulus of the hydrogels (Fig. 2A) increased first from 1.6 kPa to 6.0 kPa and further increased to 25.0 kPa along with the increase in PEGDA concentration due to the enhanced crosslinking density. In contrast, the ESR of the 9 hydrogels was correlated to the crosslinking density of the matrix network and its mechanical properties[28]. The swelling ratio declined significantly along with the increase in the PEGDA concentration (Fig. 2B). The minor difference in gelatin concentration did not affect the swelling ratio and mechanical properties of the hydrogels[29, 30].

As shown in Fig. 2C, in general, all hydrogels exhibited a similar interconnected porous structure after freeze drying. In the hydrogels with lower content of PEDGA and GelMA, the pores were small and dense. However, the pores became larger and looser with the increasing content of PEGDA and GelMA. The observed differences in the pore structure were mainly attributed to the diverse phase separation process and collapse of a portion of the polymer network during the freeze drying process. The different pore structures may contribute to different adhesive ligands and hydrogel stiffness as well.

3.2 A range of ECM adhesion can be obtained by varying the GelMA content in PEGDA/GelMA hydrogels

By varying the feeding ratio of GelMA, the number of adhesive ligands in the hydrogels was modulated. To determine the density of the adhesion ligands, osteoblastic hFOB1.19 cells were seeded on the surface of the nine PEGDA/GelMA hydrogels, and cell adhesion was detected after 24 h. As shown in Fig. 2D, more live cells (green) and fewer dead cells (red) were found on the hydrogels with higher GelMA concentrations for osteoblasts. Especially, clusters were formed on the hydrogels with 0.5% GelMA content. On the scaffolds with the same GelMA concentration, there is no significant difference in the cell adhesion among the hydrogels induced by varying the PEGDA content. Based on the calculation, the cell adhesion area was sustainably augmented with an increase in GelMA ($P<0.05$) for both cell

types (Fig. 2E). The results demonstrated that the cell adhesion affinities of PEGDA/GelMA were correlated with the GelMA content and such correlation was independent of the PEGDA concentration. Thus, we used L, M and H to represent the hydrogels with low (0.05% GelMA), middle (0.2% GelMA) and high (0.5% GelMA) adhesion ligand density (Fig. 1A, Table 1, Fig. 2D-E).

3.3 Intrascaffold-cultured osteosarcoma cells are more sensitive to matrix stiffness, while osteoblasts are more dependent on adhesion ligands

Since 3D culture resulted in cells more similar to those growing in vivo [31], we developed the intra-scaffold-cultured system for osteosarcoma cells and osteoblasts. The MTT analysis and viability assay were performed to evaluate the proliferation and viability, respectively, of the cells inside the hydrogels. Cells in the same group proliferated in a time-dependent manner (Fig. 3A-B). For osteosarcoma MG63 cells cultured within scaffolds at the same time point, fewer dead cells and more live cells were present in stiffer hydrogels (Fig. 3C). However, in hydrogels with the same stiffness, cell viability changed little when ECM adhesion ligand density varied. In contrast, the cell viability and proliferation of osteoblastic hFOB1.19 cells were correlated with the density of adhesion ligands rather than with ECM rigidity (Fig. 3D). UV cross-linking does not affect the cell viability, as indicated by little difference in the viability of the osteosarcoma cells and osteoblasts before and after UV irradiation (Fig. S2).

The tumorigenesis of MG63 cells inside the 9 hydrogels with different ECM adhesivity and rigidity were evaluated. HIFA and VEGF are both important mediators of tumor angiogenesis[11, 32]. The matrix metalloproteinase (MMP) family contributes to the formation of microenvironments that promote tumorigenesis in the early stages, particularly MMP2 and MMP9[11]. The levels of tumorigenic genes (*HIFA*, *VEGF*, *MMP2* and *MMP9*) varied with the increase in PEGDA and the resultant increase in the ECM stiffness (Fig. 4A). The expression of these genes all peaked at 25 kPa. However, in the scaffolds with the same stiffness, there was little difference. The results were further confirmed by western blot of HIFA, VEGF, MMP2 and MMP9 (Fig. 4B) and immunofluorescence staining. As shown in Fig. S3A, more cells with stronger positive MMP2 and MMP9 staining were present in the osteosarcoma cells within the more rigid hydrogels than in those within the softer hydrogels. However, in the hydrogels with the same stiffness, positive staining and cell numbers varied little with the change in the density of adhesion ligands. ALDH plays a vital role in clinical osteosarcoma metastasis[24], and CD133 is also an osteosarcoma marker of metastasis and invasion[33, 34]. As shown in Fig. 4C, the osteosarcoma cells excreted more ALDH in stiffer scaffolds, independently from ECM adhesion. Meanwhile, intracellular CD133 staining was intensified with the increase in stiffness, although it did not change much with the ECM adhesion ligand density (Fig. 4D).

In contrast to tumorigenesis of osteosarcoma cells, the indicators of osteogenic differentiation (*ALP*, *COL1*, *BMP2* and *RUNX2*)[26] in osteoblasts cultured within scaffolds were augmented with the increase in adhesion ligands rather than stiffness (Fig. 4E). Immunofluorescent staining of OCN and ALP, which are osteogenic differentiation markers, showed that positive staining was correlated with the changes in ECM adhesivity

rather than in stiffness (Fig. S3B). Western blot of ALP, COL1, BMP2 and RUNX2 (Fig. 4F) and ALP activity also confirmed that osteogenesis varied with ECM adhesion ligand density (Fig. 4G). Positive alizarin red staining, indicative of osteoblast calcification nodules, became stronger with the increase in ECM adhesion ligand density (Fig. 4H).

To further verify the *in vitro* findings, we investigated the effect of matrix stiffness and adhesion ligands on the tumorigenicity and osteogenesis *in vivo* based on subcutaneously injected MG63 cells and hFOB1.19 cells in the nude mice with PEGDA-GelMA hydrogels as vehicles. As shown in Fig. 5A-D and Table 2, the volume of osteosarcoma harvested from nude mice increased with the increase of ECM stiffness, while the tissue formed by osteoblasts enlarged with the increase of ECM adhesivity. Under the same stiffness, the osteosarcoma volume varied little with the change of ECM adhesivity. Similarly, neo-tissue formed by osteoblasts changed minimally with ECM rigidity. This was further confirmed by histological and immunohistochemical staining. As shown in Fig. 5E-F, the number of blood vessels, the percentage of necrosis area as well as the number of round, polygonal and fusiform like cells, indicative of tumor malignancy, increased with the ECM stiffness rather than with the adhesivity in osteosarcoma. In contrast, more mature and differentiated osteoblasts as indicated by eosin staining were present in the adhesive ligand rich groups for osteoblastic-like tissues. As reflected in Fig.5G-H, CD133 positive staining was intensified with the stiffness of scaffold in osteosarcoma, while OCN positive staining was strengthened with the ECM adhesivity for osteoblasts.

3.4 ECM stiffness affects osteosarcoma cells by regulating the integrin-mediated FA signaling pathway, while ECM adhesion impacts osteoblasts via the integrin-mediated AJ signaling pathway

Integrin-mediated AJ and FA signaling pathways are associated with cell-cell adhesion and mechanotransduction, respectively. As shown in Fig. 6A-B, the expression of integrin-β (ITGB) and FA signaling pathway protein (including talin-1 (TLN1), FAK, paxillin (PXN) and vinculin (VCL)) in osteosarcoma MG63 cells embedded in the 9 scaffolds was higher in the rigid hydrogels than in the flexible hydrogels. However, the expression of the AJ signaling pathway protein α-E-catenin (CTNNA1) was degraded in the rigid hydrogels than in the soft ones ($P<0.05$), which is in contrast to β-catenin (CTNNB1) expression, indicating no correlation between ECM stiffness and AJ signaling.

In contrast, the expression of the ITGB and AJ signaling pathway proteins CTNNA1 and CTNNB1 varied with scaffold adhesivity rather than with the stiffness in the intrascaffold-cultured osteoblasts ($P<0.001$), as shown in Fig. 6C-D. However, TLN1, PXN, FAK and VCL, which are key proteins in the FA signaling pathway, showed no significant differences in all the osteoblast groups.

We further examined tumorigenesis when FAK was inhibited using PF-573228. As a result of FAK inhibition, the expression of the tumorigenesis-related markers *MMP2* and *VEGF* was downregulated in the intrascaffold-cultured osteosarcoma cells compared with the unsuppressed cells, which was unanimous with the *FAK* expression (Fig. 7A). In addition, these genes exhibited no correlation with stiffness. ALDH activity also confirmed the same

results (Fig. 7B). Negative CD133 staining was also observed in blocked osteosarcoma cells cultured inside the scaffolds (Fig. 7C).

By using SHE78–7 anti-E–cadherin antibody, osteogenesis markers such as *ALP* and *OCN* were also found to drop after *CTNNA1* was blocked in the intrascaffold-cultured osteoblasts (Fig. 7D). As shown in Fig. 7E, the ALP activity of osteoblasts was also restrained with the suppression of *CTNNA1*. No significant differences were identified among the groups with different ECM adhesion ligand densities. Meanwhile, the secretion of mineralized nodules by the osteoblasts was also inhibited, as shown by mostly negative alizarin red staining in all the osteoblast groups (Fig. 7F).

3.5 Both surface-cultured osteosarcoma cells and osteoblasts are regulated primarily by matrix adhesion through the AJ signaling pathway

Osteosarcoma MG63 cells and osteoblastic hFOB1.19 cells were cultured on the surface of nine hydrogels with different ECM adhesion densities and mechanical properties. As shown in Fig. 8 A-B, both cells proliferated with time in the same group. Cell proliferation was sustainably augmented with the increase in the GelMA content ($P<0.05$) for both surface-cultured osteosarcoma MG63 cells and osteoblast hFOB1.19 cells. However, little difference was found on the scaffolds with the same GelMA content. The results were also confirmed by live/dead cell assays (Fig. S4). After 7 days of culture, it was observed that hydrogels with more GelMA content supported more live cells and fewer dead cells than those with a lower proportion of GelMA for both MG63 cells (Fig. S4A) and osteoblasts (Fig. S4B). Clusters were formed on the surface with excessive GelMA content. In contrast, the PEG content had a little effect on the cell adhesion at the same GelMA concentration.

As shown in Fig. 8C, the gene expression of *HIFA*, *VEGF*, *MMP2* and *MMP9*, which are tumorigenesis markers, in the MG63 cells cultured on the scaffold surfaces, was continuously upregulated with the increase in the ECM adhesion ($P<0.001$). In the scaffolds with the same adhesivity, there were no significant differences among the hydrogels of different rigidities ($P>0.05$). Osteoblasts responded in the same manner as osteosarcoma cells to the variations in the scaffolds. The expression of *ALP*, *COL1*, *BMP2* and *RUNX2,* which are osteogenic differentiation markers[26], was dependent on the density of GelMA rather than the stiffness (Fig. 8D).

Immunostaining of critical tumor formation and osteogenic differentiation proteins also confirmed the RT-PCR results. As shown in Fig. 8E, the positive staining of MMP2 and MMP9 in the osteosarcoma MG63 cells intensified in an ECM adhesion-dependent manner. For osteoblasts, staining of ALP and OCN, which are specific markers of osteoid formation and mineralization[26], became stronger with the increase in the adhesion ligands rather than in the stiffness (Fig. 8F).

As shown in Fig. 8G-H, the levels of ITGB, CTNNA1 and CTNNB1 for both surface-cultured osteosarcoma cells (Fig. 8G) ($P<0.05$) and osteoblasts (Fig. 8H) ($P<0.05$) increased with the adhesion ligand density, similar to those in the osteoblasts embedded in the hydrogels (Fig. 6C-D). However, the expression of key FA signaling pathway proteins had

no direct correlation with the ECM stiffness or adhesion ligand density for both osteosarcoma cells and osteoblasts cultured on the scaffold surfaces.

4. Discussion

To study the different cellular responses, we fabricated hydrogels with a cross-linked network of PEGDA and GelMA, which allowed for independent control of the compression modulus and adhesion ligand density. Engler et al. proved that relatively soft hydrogels (0.1–10 kPa) induced neurogenesis, and stiff hydrogels (25–40 kPa) promoted osteogenesis[5]. In our study, the scaffold stiffness was controlled by adjusting the PEGDA concentration in a range of 1.6 ~ 25 kPa (Table 1, Fig. 1A) and the cell adhesion ligand density, i.e., gelatin density was adjusted by varying the concentration of GelMA in the hydrogels. Due to the very low GelMA concentration compared to that of PEGDA, the impact of different GelMA concentrations on the stiffness of the obtained hydrogels should be negligible. On the other hand, by varying GelMA content, adhesion ligand density was altered, which impacted cell adhesion affinity (Fig. 2, S4). Thus, PEGDA/GelMA hydrogels provide a favorable model system to investigate the impact of individual physical cues on cell manner. This was similar to the studies of Tokuda et al who utilized PEG-peptide hydrogels to control the stiffness and adhesivity [35]. We demonstrated that intrascaffold-cultured osteosarcoma cells depended more on the ECM rigidity than on the adhesivity whereas normal osteoblasts showed the opposite trend. This finding is likely because osteosarcoma cells are anchorage-independent and thus might primarily be affected by ECM stiffness, while osteoblasts are anchorage-dependent and thus rely primarily on the adhesion ligands.

Differential cell behavior ranging from normal to cancerous may respond differently to substrate properties [36]. Osteosarcoma cells cultured within the scaffolds are dependent on the matrix rigidity rather than on the ECM adhesion ligands, as indicated by the increased cell growth and tumor malignancy observed in stiffer hydrogels compared with softer scaffolds (Fig. 3A, 3C, 4A-D, 5A-B, 5E, 5G, S3A). In contrast, osteoblasts were more sensitive to the adhesion ligands in the matrix, evidenced by the enhanced osteoblastic formation and calcification in GelMA-rich scaffolds (Fig. 3B, 3D, 4E-H, 5C-D, 5F, 5H, S3B). Variations in the cellular response of osteosarcoma cells cultured within the scaffolds indicated that cancer cells regain their anchorage-independence state in microenvironments mimicking the ECM of natural tumors. Although the adhesion ligands affect sarcoma regeneration, their impact is smaller than the effect of mechanical properties. This was not in agreement with the findings of Caliari et al, who found that ECM stiffness affected the osteogenic differentiation of MSCs [37] and those of Taubenberger et al, who found that ECM modulated cancer cell invasion [38]. This may be because the scaffolds they used were not controlled precisely with independent stiffness and adhesive ligands.

The response of cancer cells to the scaffolds differed from that of normal cells, and is likely associated with the regulation of the integrin-mediated FA signaling pathway[39] (Fig. 9). Integrin-β, an important ECM receptor, plays a critical part in mechanotransduction[40]. The coupling of integrins to F-actin[41] through talin is highly associated with integrin activation, which is essential for mechano-signaling and cancer cell function[42]. Following the formation of the integrin/talin link, signaling competent adapter proteins like paxillin

participated in the mechanical signal transduction [16]. Vinculin is an important molecule that stabilizes FAs and modulates force transmission[43]. Studies have reported that stress stimulates the combined expression of vinculin and paxillin, thereby activating FAK[18, 19, 44] to eventually promote the expression of tumor malignancy markers, such as MMP2, MMP9 and VEGF[45]. During mechanotransduction, the Wnt-independent activation of β-catenin is also initiated by FAK upregulation[46] to increase MMP2 and MMP9 activity, thereby contributing to tumorigenesis[47]. FAK signaling pathway also regulates cancer malignancy by modulating ALDH[48] and CD133[49]. In this study, intrascaffold-cultured MG63 cells were predominantly affected by ECM stiffness, which may be regulated through the integrin-mediated FA signaling pathway (Fig. 6A-B, 7A-C), as evidenced by the association of crucial FA molecule expression with matrix rigidity (Fig. 7A-C). However, adhesion ligands have only a minor effect on the intrascaffold-cultured osteosarcoma cells, as indicated by the independence of integrin-mediated malignancy and the expression of α-E-catenin and β-catenin upon ECM adhesion (Fig. 6A-B). This phenomenon mirrors the earlier finding that α-E-catenin expression is not associated with the ECM adhesion in cancer[50]. Studies have also shown that AJ proteins are downregulated in the cancer cells[15], suggesting that cancer cells do not require attachment. Thus, cancer cells, which gradually lose AJ protein expression[51], may not be as sensitive to ECM adhesivity as normal cells.

Whether cultured inside the scaffold or on the surface, normal osteoblasts, which are likely regulated by integrin-mediated AJ signaling pathways, were more sensitive to ECM adhesion ligands than the osteosarcoma cells (Fig. 9). Integrins are heterodimeric transmembrane receptors linked to the cortical actin cytoskeleton through scaffolding proteins, thereby influencing the anchorage-dependent cells such as osteoblasts. Integrin-β binding to α-E-catenin and β-catenin contributes to the anchorage dependency. For both intrascaffold- and surface-cultured osteoblasts, the scaffolds supported the cell growth in a GelMA-dependent manner (Fig. 3B, 3D, 4D-F, 8B, 8D, 8F, S3B, S4B), which is consistent with the increase in the adhesion molecule expression, including α-E-catenin and β-catenin (Fig. 6C-D, 7D-F, 8H). This finding indicates that adhesion ligands exert a major effect on the anchorage-dependent osteoblasts through modulating the integrin-mediated AJ signaling pathway.

Intriguingly, osteosarcoma cells behave differently on the scaffold surfaces compared with those embedded in the scaffolds, which are more influenced by ECM adhesion than stiffness. When cultured on the scaffold surfaces, the osteosarcoma cells reacted to the matrix in a similar manner as the osteoblasts. For anchorage-independent cancer cells, they are “forced” to attach to the flat surface of the substrate and have to adopt unnatural characteristics, such as an aberrant flattened morphology, which might hamper cell proliferation[52] and change the biological properties, functions and even genetic characteristics of the cells[53–56]. In particular, surface culture is similar to the monolayer culture, which renders cancer cells sensitive to apoptosis and results in the expression of fewer genes conferring tumor malignancy[57]. Thus, cancer cells behave similarly to anchorage-dependent cells and tend to rely on the AJ signaling pathway when they are flattened onto a substrate. This also demonstrated that 3D culture was more suitable for tumor and tissue development [31].

In conclusion, by independently changing the PEGDA and GelMA in the PEDA/GelMA hydrogels, we achieved crosslinked matrix with independently tunable stiffness (1.6, 6 and 25 kPa for 5%, 10%, 15% PEDGA, respectively) and adhesion ligand density (low, medium and high for 0.05%, 0.2%, 0.5% GelMA respectively). By studying the response of cells to such tunable hydrogels, we observed that ECM stiffness rather than matrix adhesivity affects the growth and progression of the intrascaffold-cultured osteosarcoma cells through regulating the integrin-mediated FA signaling pathway. On the contrary, their normal counterparts (osteoblasts) are mainly affected by ECM adhesion ligands through modulating the integrin-mediated AJ signaling pathway. This study may provide strategies for tailoring scaffolds for generating in vitro tumor models to test anticancer therapeutics and for regenerating tissue to repair defects.

Supplementary Material

Refer to Web version on PubMed Central for supplementary material.

Acknowledgments

This work has been financially supported by the National Key R&D Program of China (2016YFB0700804 and 2016YFA0100900), Guangxi Scientific Research and Technological Development Foundation (GuikeAB16450003), Guangxi high school innovative team and distinguished scholars program (The third batch), Distinguished Young Scholars Program of Guangxi Medical University, Guangxi Science Fund for Distinguished Young Scholars (2014GXNSFGA118006), Innovation Project of Guangxi Graduate Education (YCSZ2015108), the National Natural Science Foundation of China (51673171 and 51673168), Innovation Project of Collaborative Innovation Center of Guangxi Biological Medicine for Graduate Students, and Zhejiang Provincial Natural Science Foundation of China (LZ16E030001). YZ and CBM also acknowledge the financial support from National Institutes of Health (CA200504 and CA195607),

References

[1]. Borghi N, Lowndes M, Maruthamuthu V, Gardel ML, Nelson WJ. Regulation of cell motile behavior by crosstalk between cadherin- and integrin-mediated adhesions. Proceedings of the National Academy of Sciences of the United States of America 2010;107:13324–9. [PubMed: 20566866]

[2]. Yi H, Zeng D, Shen Z, Liao J, Wang X, Liu Y, et al. Integrin alphavbeta3 enhances beta-catenin signaling in acute myeloid leukemia harboring Fms-like tyrosine kinase-3 internal tandem duplication mutations: implications for microenvironment influence on sorafenib sensitivity. Oncotarget 2016.

[3]. Hynes RO. Integrins: versatility, modulation, and signaling in cell adhesion. Cell 1992;69:11–25. [PubMed: 1555235]

[4]. Miyamoto S, Teramoto H, Coso OA, Gutkind JS, Burbelo PD, Akiyama SK, et al. Integrin function: molecular hierarchies of cytoskeletal and signaling molecules. J Cell Biol 1995;131:791–805. [PubMed: 7593197]

[5]. Engler AJ, Sen S, Sweeney HL, Discher DE. Matrix elasticity directs stem cell lineage specification. Cell 2006;126:677–89. [PubMed: 16923388]

[6]. Han J, Xie C, Pei T, Wang J, Lan Y, Huang K, et al. Deregulated AJAP1/beta-catenin/ZEB1 signaling promotes hepatocellular carcinoma carcinogenesis and metastasis. Cell death & disease 2017;8:e2736. [PubMed: 28383563]

[7]. Kawada M, Yamagoe S, Murakami Y, Suzuki K, Mizuno S, Uehara Y. Induction of p27Kip1 degradation and anchorage independence by Ras through the MAP kinase signaling pathway. Oncogene 1997;15:629–37. [PubMed: 9264403]

[8]. Paszek MJ, Zahir N, Johnson KR, Lakins JN, Rozenberg GI, Gefen A, et al. Tensional homeostasis and the malignant phenotype. Cancer cell 2005;8:241–54. [PubMed: 16169468]

[9]. Hirata E, Girotti MR, Viros A, Hooper S, Spencer-Dene B, Matsuda M, et al. Intravital imaging reveals how BRAF inhibition generates drug-tolerant microenvironments with high integrin beta1/FAK signaling. Cancer Cell 2015;27:574–88. [PubMed: 25873177]

[10]. Ananthanarayanan B, Kim Y, Kumar S. Elucidating the mechanobiology of malignant brain tumors using a brain matrix-mimetic hyaluronic acid hydrogel platform. Biomaterials 2011;32:7913–23. [PubMed: 21820737]

[11]. Ghosh A, Dasgupta D, Ghosh A, Roychoudhury S, Kumar D, Gorain M, et al. MiRNA199a-3p suppresses tumor growth, migration, invasion and angiogenesis in hepatocellular carcinoma by targeting VEGFA, VEGFR1, VEGFR2, HGF and MMP2. Cell death & disease 2017;8:e2706. [PubMed: 28358369]

[12]. Kenny PA, Lee GY, Myers CA, Neve RM, Semeiks JR, Spellman PT, et al. The morphologies of breast cancer cell lines in three-dimensional assays correlate with their profiles of gene expression. Mol Oncol 2007;1:84–96. [PubMed: 18516279]

[13]. Shields JD, Emmett MS, Dunn DB, Joory KD, Sage LM, Rigby H, et al. Chemokine-mediated migration of melanoma cells towards lymphatics--a mechanism contributing to metastasis. Oncogene 2007;26:2997–3005. [PubMed: 17130836]

[14]. Nguyen-Ngoc KV, Cheung KJ, Brenot A, Shamir ER, Gray RS, Hines WC, et al. ECM microenvironment regulates collective migration and local dissemination in normal and malignant mammary epithelium. Proceedings of the National Academy of Sciences of the United States of America 2012;109:E2595–604. [PubMed: 22923691]

[15]. Chaudhuri O, Koshy ST, Branco da Cunha C, Shin JW, Verbeke CS, Allison KH, et al. Extracellular matrix stiffness and composition jointly regulate the induction of malignant phenotypes in mammary epithelium. Nature materials 2014;13:970–8. [PubMed: 24930031]

[16]. Hytonen VP, Wehrle-Haller B. Mechanosensing in cell-matrix adhesions - Converting tension into chemical signals. Exp Cell Res 2016;343:35–41. [PubMed: 26518118]

[17]. Goult BT, Zacharchenko T, Bate N, Tsang R, Hey F, Gingras AR, et al. RIAM and vinculin binding to talin are mutually exclusive and regulate adhesion assembly and turnover. The Journal of biological chemistry 2013;288:8238–49. [PubMed: 23389036]

[18]. Turner CE, Glenney JR, Jr., Burridge K Paxillin: a new vinculin-binding protein present in focal adhesions. The Journal of cell biology 1990;111:1059–68. [PubMed: 2118142]

[19]. Schrader J, Gordon-Walker TT, Aucott RL, van Deemter M, Quaas A, Walsh S, et al. Matrix stiffness modulates proliferation, chemotherapeutic response, and dormancy in hepatocellular carcinoma cells. Hepatology 2011;53:1192–205. [PubMed: 21442631]

[20]. Li P, Dou X, Feng C, Schonherr H. Enhanced cell adhesion on a bio-inspired hierarchically structured polyester modified with gelatin-methacrylate. Biomaterials science 2018;6:785–92. [PubMed: 29210373]

[21]. Yang X, Sarvestani SK, Moeinzadeh S, He X, Jabbari E. Three-dimensional-engineered matrix to study cancer stem cells and tumorsphere formation: effect of matrix modulus. Tissue engineering Part A 2013;19:669–84. [PubMed: 23013450]

[22]. Maubant S, Saint-Dizier D, Boutillon M, Perron-Sierra F, Casara PJ, Hickman JA, et al. Blockade of alpha v beta3 and alpha v beta5 integrins by RGD mimetics induces anoikis and not integrin-mediated death in human endothelial cells. Blood 2006;108:3035–44. [PubMed: 16835373]

[23]. Mejia-Rangel J, Cordova E, Orozco L, Ventura-Gallegos JL, Mitre-Aguilar I, Escalona-Guzman A, et al. Pro-adhesive phenotype of normal endothelial cells responding to metastatic breast cancer cell conditioned medium is linked to NFkappaB-mediated transcriptomic regulation. International journal of oncology 2016;49:2173–85. [PubMed: 27666521]

[24]. Yu S, Fourman MS, Mahjoub A, Mandell JB, Crasto JA, Greco NG, et al. Lung cells support osteosarcoma cell migration and survival. BMC Cancer 2017;17:78. [PubMed: 28122543]

[25]. Tsukatani T, Matsumoto K. Flow-injection fluorometric quantification of pyruvate using co-immobilized pyruvate decarboxylase and aldehyde dehydrogenase reactor: Application to measurement of acetate, citrate and l-lactate. Talanta 2006;69:637–42. [PubMed: 18970615]

[26]. Jiang T, Zhou B, Huang L, Wu H, Huang J, Liang T, et al. Andrographolide Exerts Pro-Osteogenic Effect by Activation of Wnt/beta-Catenin Signaling Pathway in Vitro. Cellular

physiology and biochemistry : international journal of experimental cellular physiology, biochemistry, and pharmacology 2015;36:2327–39.

[27]. Van Vlierberghe S, Fritzinger B, Martins JC, Dubruel P. Hydrogel network formation revised: high-resolution magic angle spinning nuclear magnetic resonance as a powerful tool for measuring absolute hydrogel cross-link efficiencies. Appl Spectrosc 2010;64:1176–80. [PubMed: 20925989]

[28]. Slaughter BV, Khurshid SS, Fisher OZ, Khademhosseini A, Peppas NA. Hydrogels in regenerative medicine. Adv Mater 2009;21:3307–29. [PubMed: 20882499]

[29]. Ping S, Liu S, Zhou Y, Li Z, Li Y, Liu K, et al. Protein disulfide isomerase-mediated apoptosis and proliferation of vascular smooth muscle cells induced by mechanical stress and advanced glycosylation end products result in diabetic mouse vein graft atherosclerosis. Cell death & disease 2017;8:e2818. [PubMed: 28542133]

[30]. Liu M, Zeng X, Ma C, Yi H, Ali Z, Mou X, et al. Injectable hydrogels for cartilage and bone tissue engineering. Bone Res 2017;5:17014. [PubMed: 28584674]

[31]. Bray LJ, Binner M, Korner Y, von Bonin M, Bornhauser M, Werner C. A three-dimensional ex vivo tri-culture model mimics cell-cell interactions between acute myeloid leukemia and the vascular niche. Haematologica 2017;102:1215–26. [PubMed: 28360147]

[32]. Li F, Mei H, Gao Y, Xie X, Nie H, Li T, et al. Co-delivery of oxygen and erlotinib by aptamer-modified liposomal complexes to reverse hypoxia-induced drug resistance in lung cancer. Biomaterials 2017;145:56–71. [PubMed: 28843733]

[33]. Ni M, Xiong M, Zhang X, Cai G, Chen H, Zeng Q, et al. Poly(lactic-co-glycolic acid) nanoparticles conjugated with CD133 aptamers for targeted salinomycin delivery to CD133+ osteosarcoma cancer stem cells. Int J Nanomedicine 2015;10:2537–54. [PubMed: 25848270]

[34]. Zhang N, Zhang R, Zou K, Yu W, Guo W, Gao Y, et al. Keratin 23 promotes telomerase reverse transcriptase expression and human colorectal cancer growth. Cell death & disease 2017;8:e2961. [PubMed: 28749462]

[35]. Tokuda EY, Jones CE, Anseth KS. PEG-peptide hydrogels reveal differential effects of matrix microenvironmental cues on melanoma drug sensitivity. Integrative biology : quantitative biosciences from nano to macro 2017;9:76–87. [PubMed: 28001152]

[36]. Li Z, Dranoff JA, Chan EP, Uemura M, Sevigny J, Wells RG. Transforming growth factor-beta and substrate stiffness regulate portal fibroblast activation in culture. Hepatology 2007;46:1246–56. [PubMed: 17625791]

[37]. Caliari SR, Vega SL, Kwon M, Soulas EM, Burdick JA. Dimensionality and spreading influence MSC YAP/TAZ signaling in hydrogel environments. Biomaterials 2016;103:314–23. [PubMed: 27429252]

[38]. Taubenberger AV, Bray LJ, Haller B, Shaposhnykov A, Binner M, Freudenberg U, et al. 3D extracellular matrix interactions modulate tumour cell growth, invasion and angiogenesis in engineered tumour microenvironments. Acta Biomater 2016;36:73–85. [PubMed: 26971667]

[39]. Hong SG, Kim GH. Mechanically improved electrospun PCL biocomposites reinforced with a collagen coating process: preparation, physical properties, and cellular activity. Bioprocess and biosystems engineering 2013;36:205–14. [PubMed: 22763777]

[40]. Yang M, Xiao LW, Liao EY, Wang QJ, Wang BB, Lei JX. The role of integrin-beta/FAK in cyclic mechanical stimulation in MG-63 cells. International journal of clinical and experimental pathology 2014;7:7451–9. [PubMed: 25550780]

[41]. Fang KP, Dai W, Ren YH, Xu YC, Zhang SM, Qian YB. Both Talin-1 and Talin-2 correlate with malignancy potential of the human hepatocellular carcinoma MHCC-97 L cell. BMC cancer 2016;16.

[42]. Kukkurainen S, Maatta JA, Saeger J, Valjakka J, Vogel V, Hytonen VP. The talin-integrin interface under mechanical stress. Molecular bioSystems 2014;10:3217–28. [PubMed: 25277990]

[43]. Brown DT, Izard T. Vinculin-cell membrane interactions. Oncotarget 2015;6:34043–4. [PubMed: 26431280]

[44]. Hytonen VP, Wehrle-Haller B. Mechanosensing in cell-matrix adhesions - Converting tension into chemical signals. Experimental Cell Research 2016;343:35–41. [PubMed: 26518118]

[45]. Tsai HC, Tzeng HE, Huang CY, Huang YL, Tsai CH, Wang SW, et al. WISP-1 positively regulates angiogenesis by controlling VEGF-A expression in human osteosarcoma. Cell death & disease 2017;8:e2750. [PubMed: 28406476]

[46]. Du J, Zu Y, Li J, Du SY, Xu YP, Zhang L, et al. Extracellular matrix stiffness dictates Wnt expression through integrin pathway. Scientific reports 2016;6.

[47]. Bao G, Wang N, Li R, Xu G, Liu P, He B. Glycoprotein non-metastatic melanoma protein B promotes glioma motility and angiogenesis through the Wnt/beta-catenin signaling pathway. Experimental biology and medicine 2016.

[48]. VanKlompenberg MK, Bedalov CO, Soto KF, Prosperi JR. APC selectively mediates response to chemotherapeutic agents in breast cancer. BMC Cancer 2015;15:457. [PubMed: 26049416]

[49]. Wang Z, Shen M, Lu P, Li X, Zhu S, Yue S. NEDD9 may regulate hepatocellular carcinoma cell metastasis by promoting epithelial-mesenchymal-transition and stemness via repressing Smad7. Oncotarget 2017;8:1714–24. [PubMed: 27974675]

[50]. Benjamin JM, Nelson WJ. Bench to bedside and back again: molecular mechanisms of alpha-catenin function and roles in tumorigenesis. Seminars in cancer biology 2008;18:53–64. [PubMed: 17945508]

[51]. Pinheiro D, Hannezo E, Herszterg S, Bosveld F, Gaugue I, Balakireva M, et al. Transmission of cytokinesis forces via E-cadherin dilution and actomyosin flows. Nature 2017;545:103–7. [PubMed: 28296858]

[52]. Maltman DJ, Przyborski SA. Developments in three-dimensional cell culture technology aimed at improving the accuracy of in vitro analyses. Biochem Soc T 2010;38:1072–5.

[53]. Josse C, Schoemans R, Niessen NA, Delgaudine M, Hellin AC, Herens C, et al. Systematic chromosomal aberrations found in murine bone marrow-derived mesenchymal stem cells. Stem Cells Dev 2010;19:1167–73. [PubMed: 20109032]

[54]. Wang Y, Huso DL, Harrington J, Kellner J, Jeong DK, Turney J, et al. Outgrowth of a transformed cell population derived from normal human BM mesenchymal stem cell culture. Cytotherapy 2005;7:509–19. [PubMed: 16306013]

[55]. Tolar J, Nauta AJ, Osborn MJ, Panoskaltsis Mortari A, McElmurry RT, Bell S, et al. Sarcoma derived from cultured mesenchymal stem cells. Stem Cells 2007;25:371–9. [PubMed: 17038675]

[56]. Rosland GV, Svendsen A, Torsvik A, Sobala E, McCormack E, Immervoll H, et al. Long-term cultures of bone marrow-derived human mesenchymal stem cells frequently undergo spontaneous malignant transformation. Cancer Res 2009;69:5331–9. [PubMed: 19509230]

[57]. Hutmacher DW, Loessner D, Rizzi S, Kaplan DL, Mooney DJ, Clements JA. Can tissue engineering concepts advance tumor biology research? Trends Biotechnol 2010;28:125–33. [PubMed: 20056286]

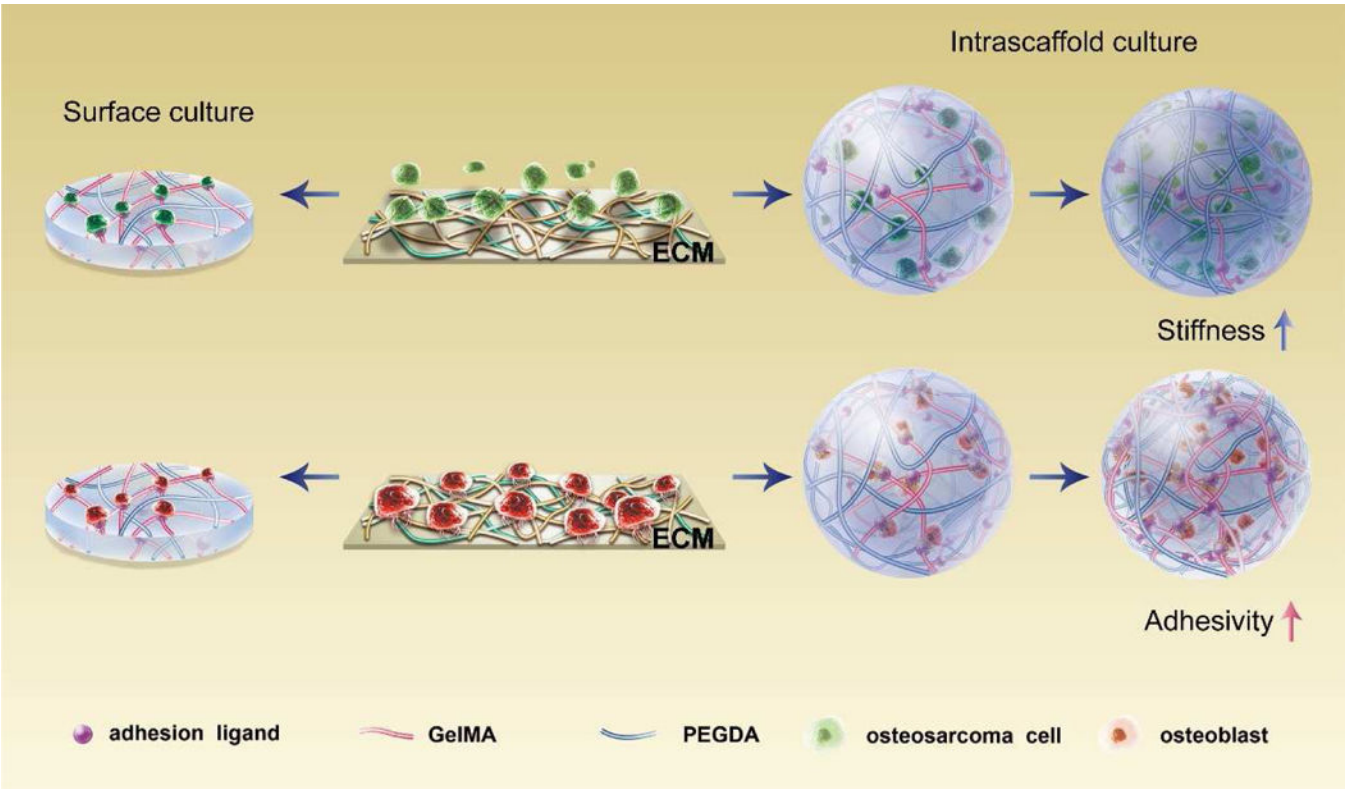

Fig. 1.

Schematic description of different cellular responses of osteosarcoma cells (anchorage independent) and osteoblasts (anchorage-dependent) to scaffold stiffness and adhesivity

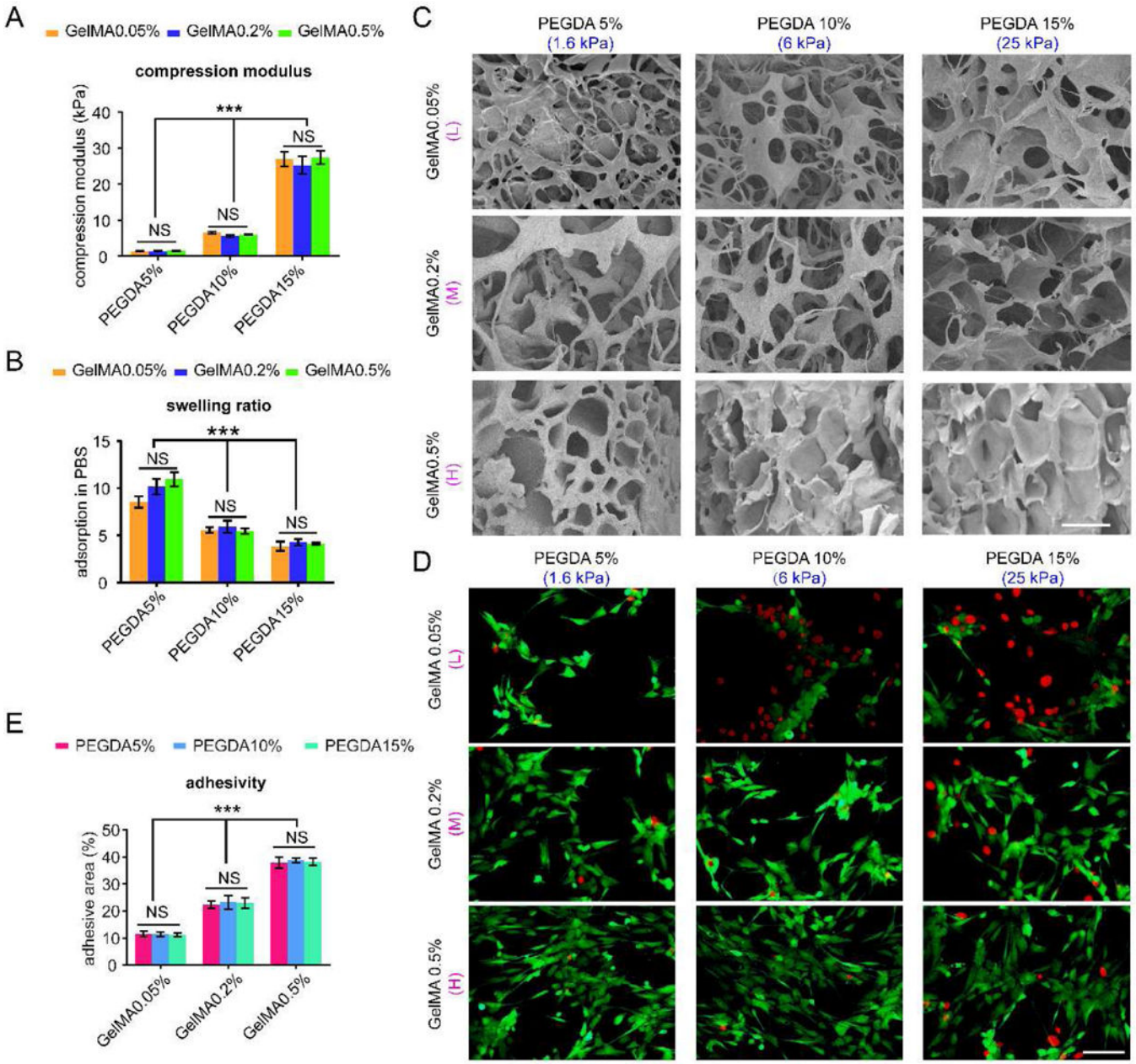

Fig. 2. Evaluation of the hydrogels.

(A) Compression modulus of 9 hydrogels after gelation, n=3. **(B)** Swelling ratio of 9 scaffolds, n=3. **(C)** SEM images of different hydrogels after freeze drying. Scale bar: 100 μm. **(D)** Representative images of osteoblasts attached on the surface of the 9 hydrogels after 24 h. Scale bar: 50 μm. **(E)** Percentage of adhesive area of osteoblasts cultured on 9 hydrogel surfaces after 24 h per view. n=10; mean ± SD; *P<0.05, **P<0.01, ***P<0.001; NS, not significant. L, M and H correspond to low (0.05% GelMA), middle (0.2% GelMA) and high (0.5% GelMA) adhesion ligand density.

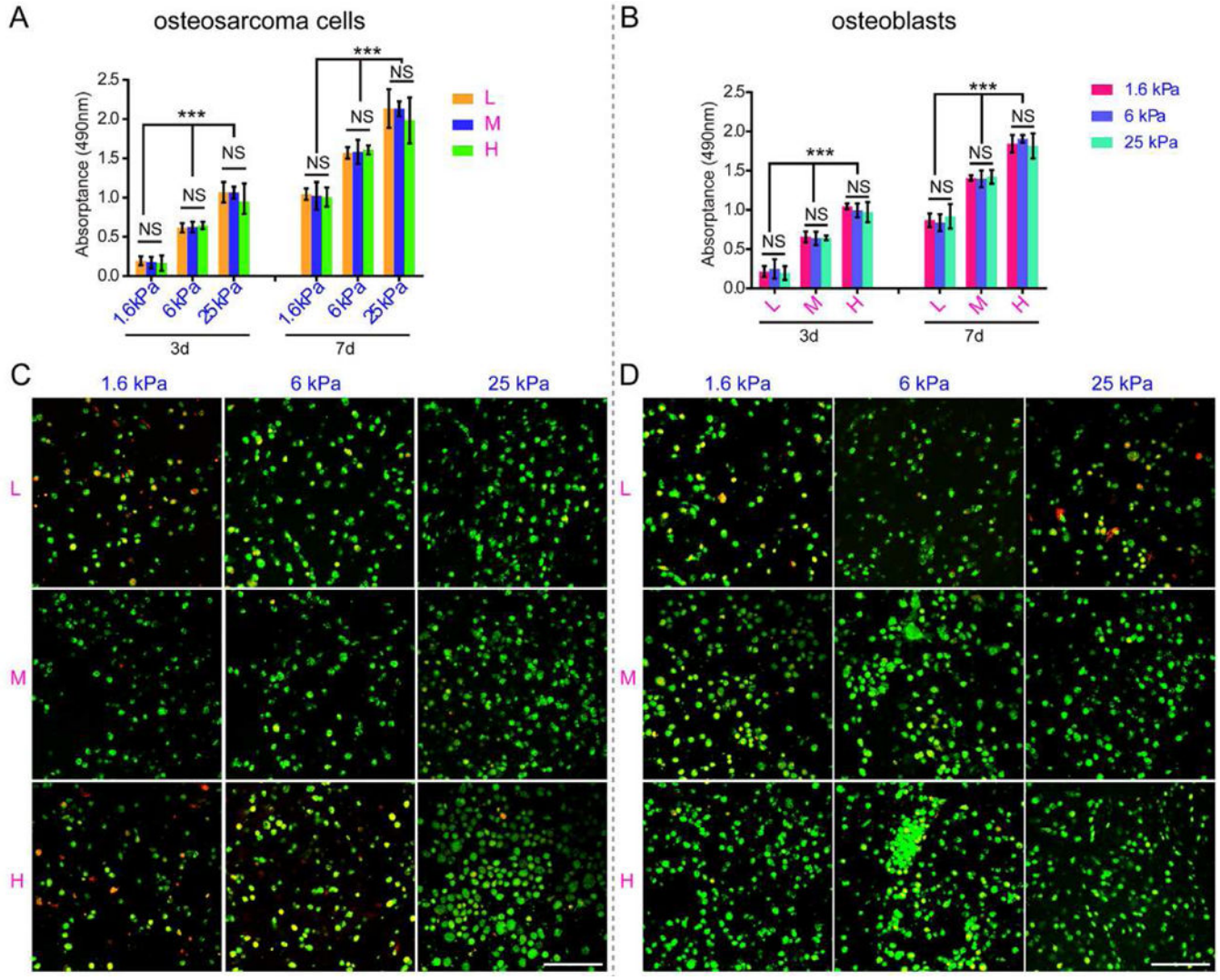

Fig. 3. Cell viability and proliferation of osteosarcoma cells and osteoblasts cultured within scaffolds.

(A) Cell proliferation of intrascaffold-cultured osteosarcoma cells after 3 and 7 days by MTT analysis. **(B)** Cell Proliferation of intrascaffold-cultured osteoblasts after 3 and 7 days by MTT analysis. **(C)** Representative images of intrascaffold-cultured osteosarcoma cells after 7 days by live/dead cell assay. Scale bar: 50 μm. **(D)** Representative images of intrascaffold-cultured osteoblasts after 7 days by live/dead cell assay. Scale bar: 50 μm. n=3; mean ± SD; *P<0.05, **P<0.01, ***P<0.001; NS, not significant. L, M and H correspond to low (0.05% GelMA), middle (0.2% GelMA) and high (0.5% GelMA) adhesion ligand density.

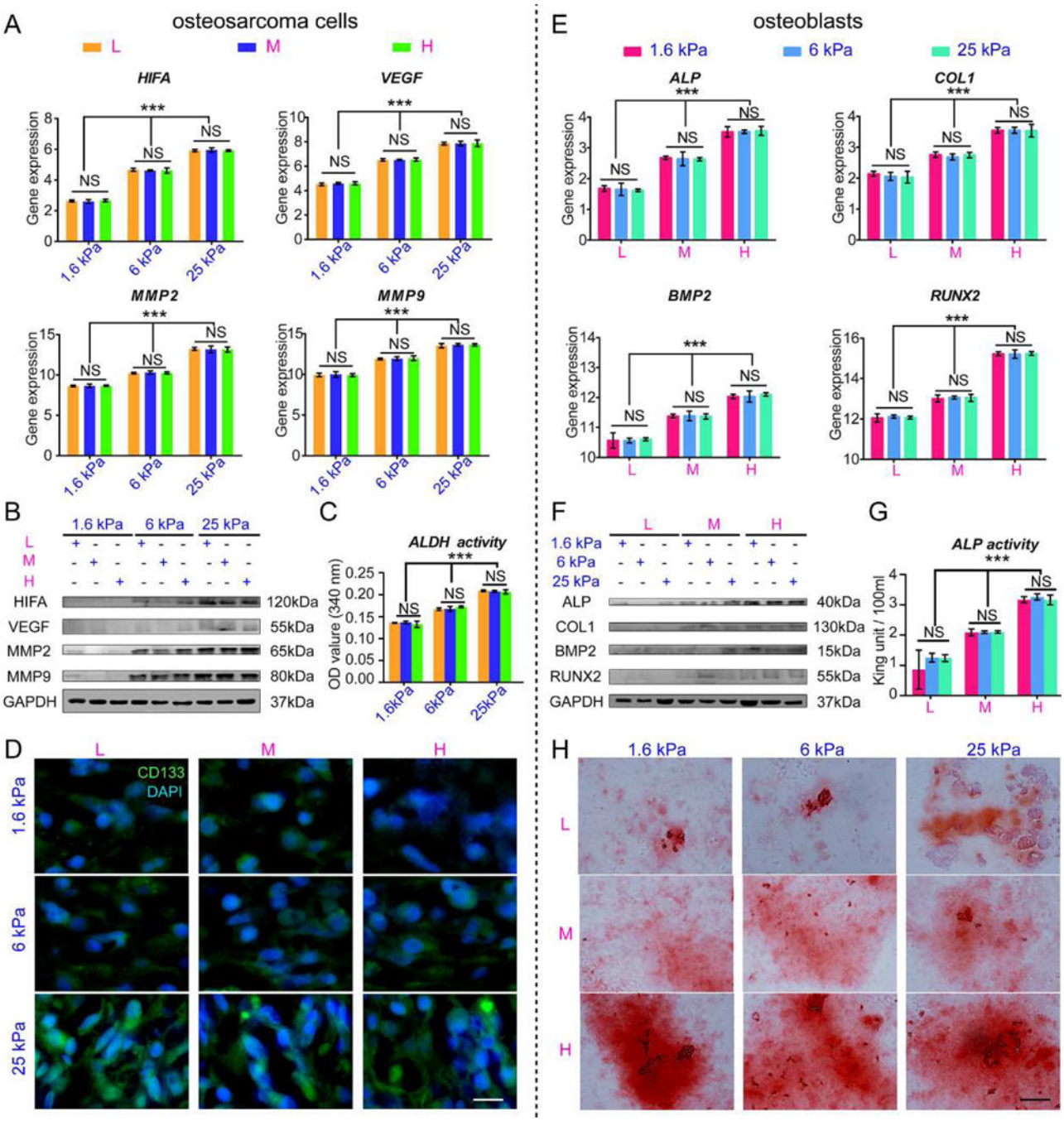

Fig. 4. The tumorigenesis of osteosarcoma cells and osteogenesis of osteoblasts cultured within scaffolds *in vitro*.

(A) *HIF*, *VEGF*, *MMP2* and *MMP9* mRNA expression in osteosarcoma cells cultured within scaffolds for 7 days. **(B)** Representative blots of HIFA, VEGF, MMP2, MMP9 and GAPDH in intrascaffold-cultured osteosarcoma cells after 7 days. **(C)** ALDH activity in intrascaffold-cultured osteosarcoma cells after 7 days. **(D)** The immunofluorescent staining of CD133 in intrascaffold-cultured osteosarcoma cells after 7 days. Scale bar: 10 μm. **(E)** *ALP*, *BMP2*, *COL1* and *RUNX2* mRNA expression in osteoblasts cultured within scaffolds

for 7 days. **(F)** Representative blots of ALP, COL1, BMP2, RUNX2 and GAPDH in intrascaffold-cultured osteoblasts after 7 days. **(G)** ALP activity of intrascaffold-cultured osteoblasts after 7 days. **(H)** Alizarin red staining of intrascaffold-cultured osteoblasts after 7 days. Scale bar: 10 μm. n=3; mean ± SD; *P<0.05, **P<0.01, ***P<0.001; NS, not significant. L, M and H correspond to low (0.05% GelMA), middle (0.2% GelMA) and high (0.5% GelMA) adhesion ligand density.

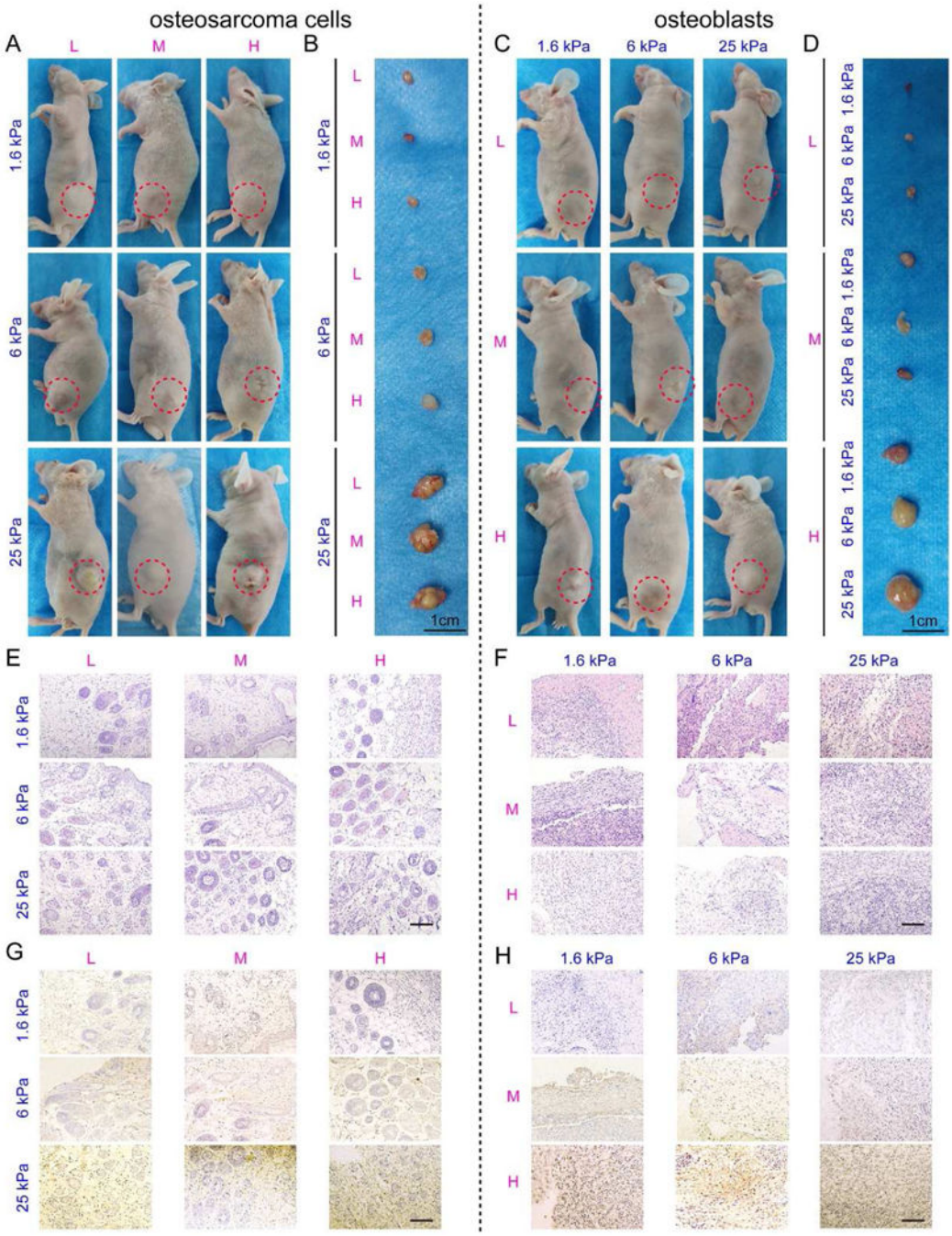

Fig. 5. The tumorigenesis of osteosarcoma cells and osteogenesis of osteoblasts cultured within the scaffolds *in vivo*.

(A-D) Representative images of nude mice and harvested samples constructed with **(A, B)** MG63 cells and **(C, D)** hFOB1.19 cells in 9 hydrogels. Red dotted circles indicate the tumor and the neoplasms. Scale bar: 1 cm. **(E-F)** HE staining of the **(E)** MG63 tumors and **(F)** hFOB1.19 neoplasms. Scale bar: 50 μm. **(G)** CD133 immunohistochemistry of the MG63 tumors. Scale bar: 50 μm. **(H)** OCN immunohistochemistry of the hFOB1.19 neoplasms. Scale bar: 50 μm.

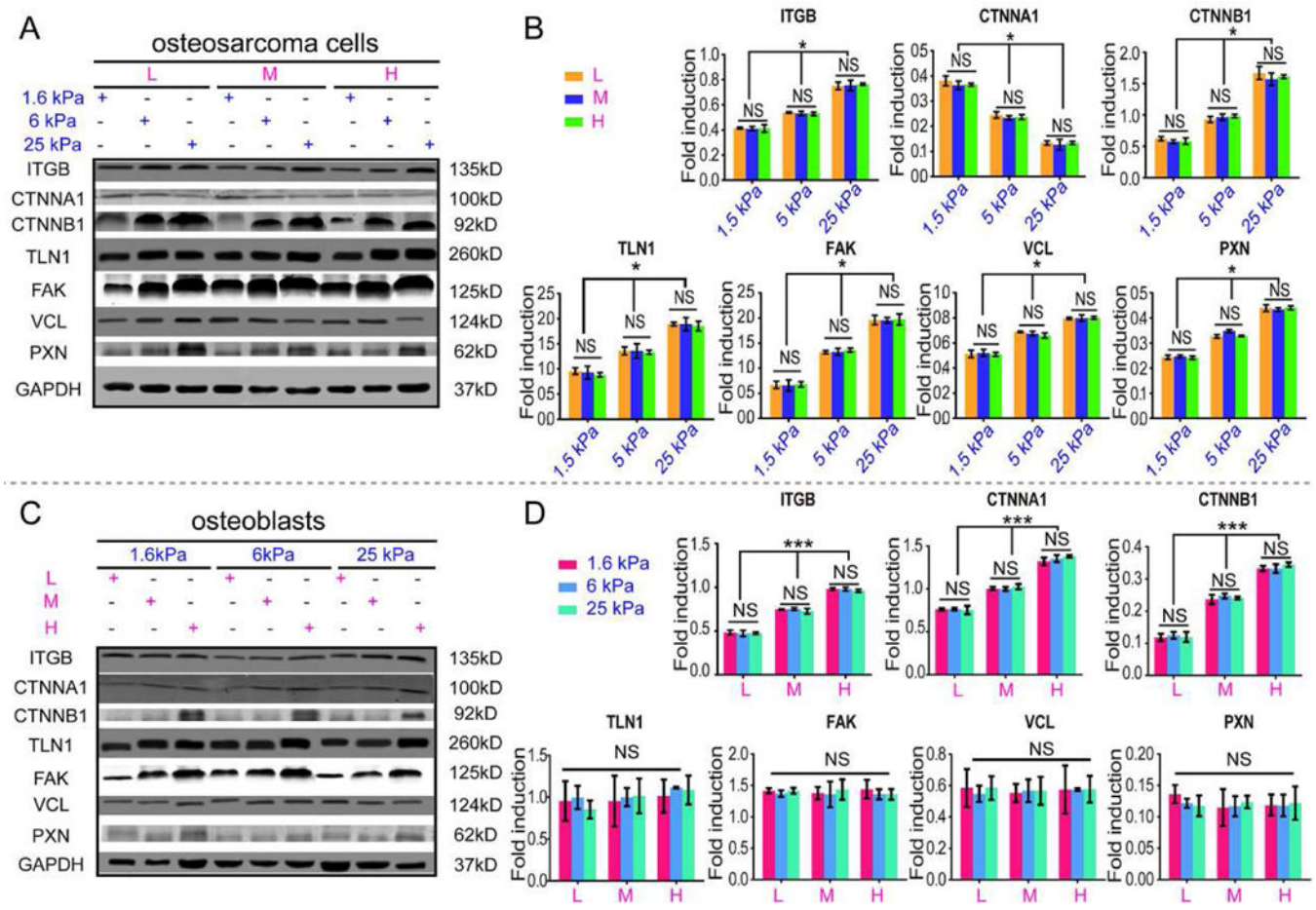

Fig. 6. Regulation of ECM on osteosarcoma and osteoblastic cells.

(A) Representative blots of ITGB, CTNNA1, CTNNB1, TLN1, FAK, VCL, PXN and GAPDH in intrascaffold-cultured osteosarcoma cells after 7 days. **(B)** Fold induction of ITGB, CTNNA1, CTNNB1, TLN1, FAK, VCL and PXN expression in intrascaffold-cultured osteosarcoma cells after 7 days. **(C)** Representative blots of ITGB, CTNNA1, CTNNB1, TLN1, FAK, VCL, PXN and GAPDH in intrascaffold-cultured osteoblasts after 7 days. **(D)** Fold induction of ITGB, CTNNA1, CTNNB1, TLN1, FAK, VCL and PXN expression in intrascaffold-cultured osteoblasts after 7 days. n=3; mean ± SD; *P<0.05, **P<0.01, ***P<0.001; NS, not significant. L, M and H correspond to low (0.05% GelMA), middle (0.2% GelMA) and high (0.5% GelMA) adhesion ligand density.

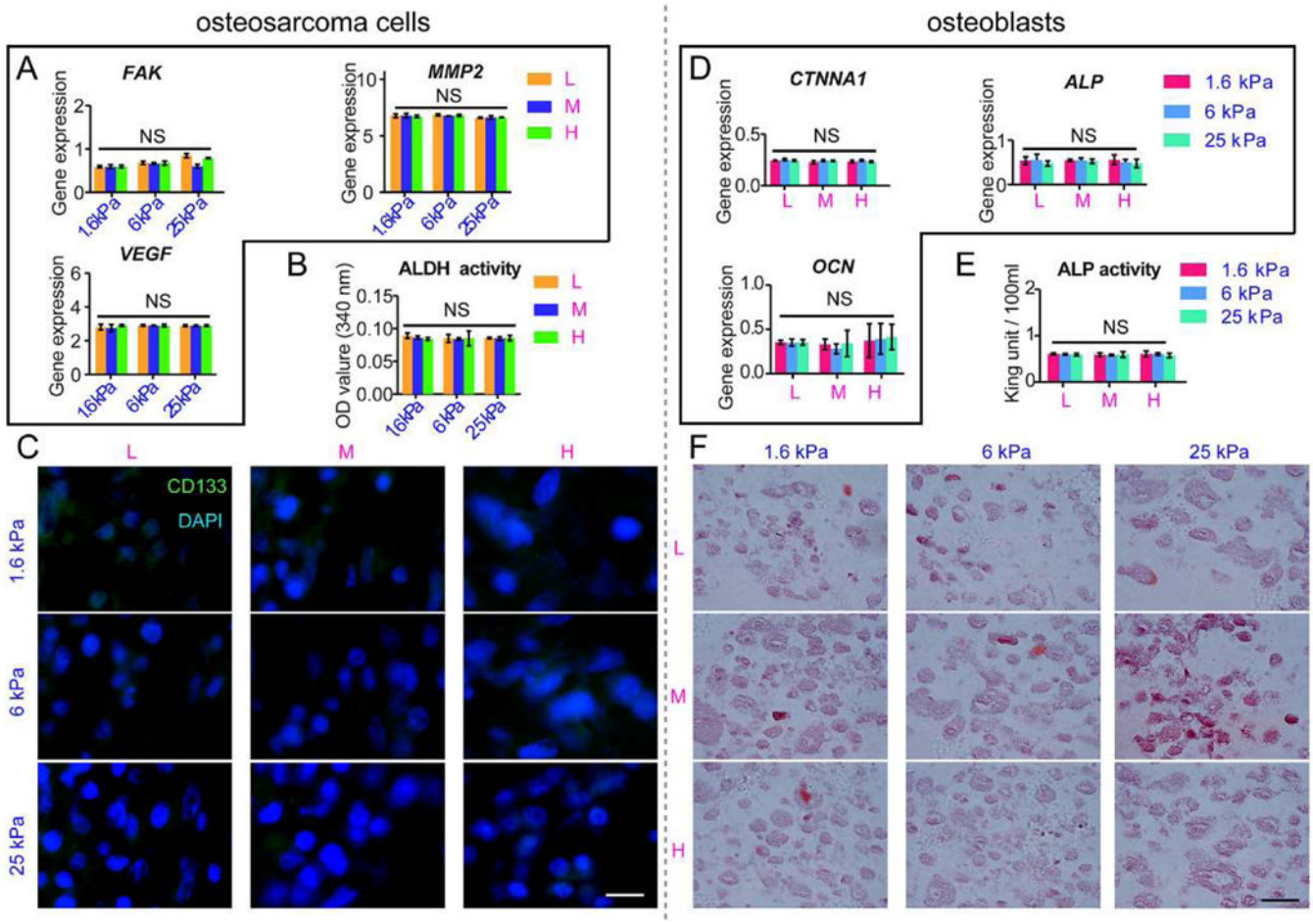

Fig. 7. Intrascaffold-cultured osteosarcoma cells were treated with FAK inhibitor of PF-573228, and intrascaffold-cultured osteoblasts were treated with SHE78–7 anti-E-cadherin antibody.

(A) *FAK*, *MMP2* and *VEGF* mRNA expression in osteosarcoma cells; **(B)** ALDH activity of osteosarcoma cells; **(C)** immunofluorescent CD133 staining in osteosarcoma cells; **(D)** *CTNNA1*, *ALP* and *OCN* mRNA expression in osteoblasts; **(E)** ALP activity of osteoblasts; **(F)** alizarin red staining in osteoblasts after 7 days. n=3; mean ± SD; *P<0.05, **P<0.01, ***P<0.001; NS, not significant. L, M and H correspond to low (0.05% GelMA), middle (0.2% GelMA) and high (0.5% GelMA) adhesion ligand density.

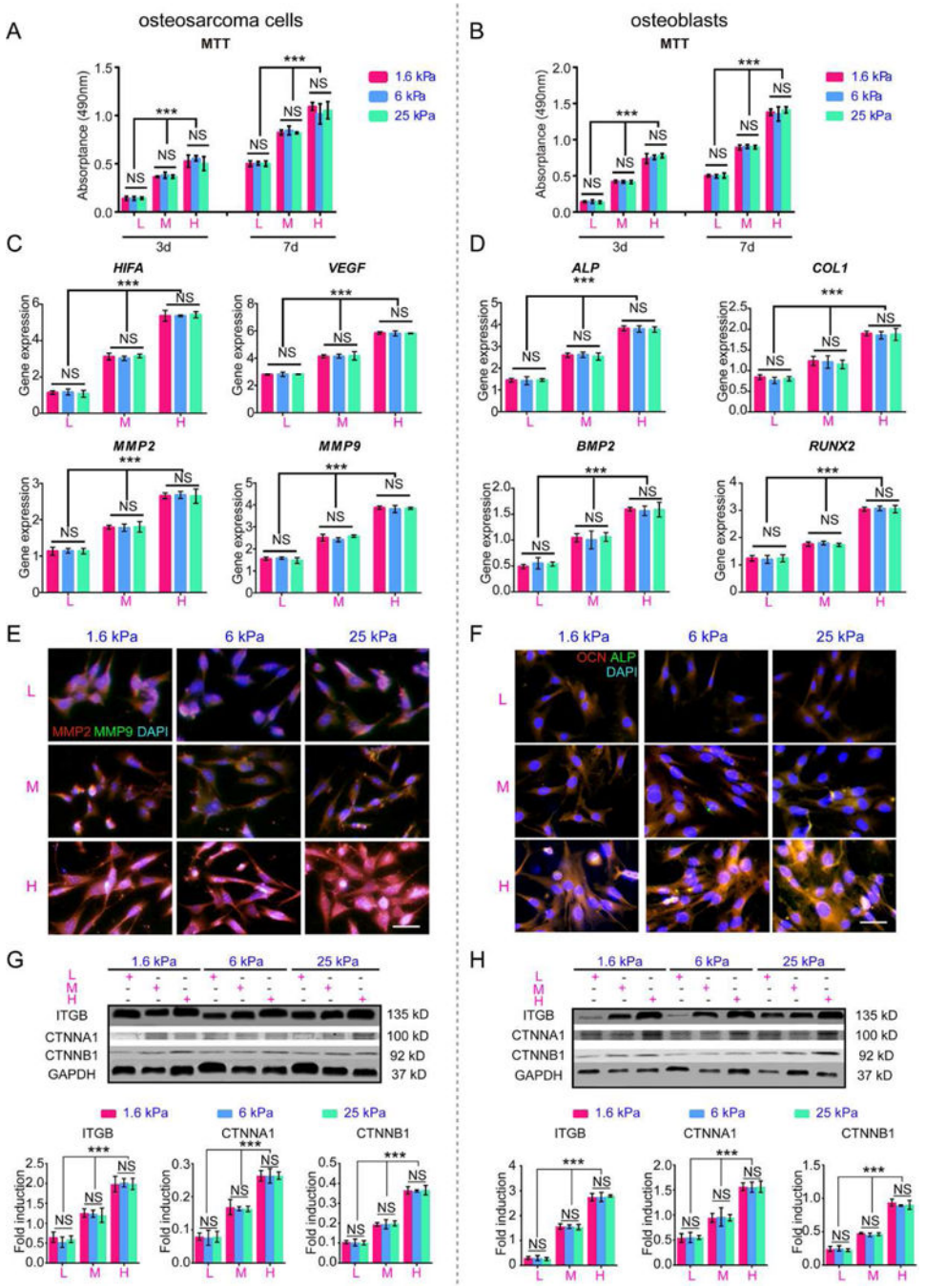

Fig. 8. Behavior of osteosarcoma cells and osteoblasts cultured on the scaffold surfaces.

(A) Cell Proliferation of surface-cultured osteosarcoma cells after 3 and 7 days. **(B)** Cell proliferation of surface-cultured osteoblasts after 3 and 7 days. **(C)** *HIF*, *VEGF*, *MMP2* and *MMP9* mRNA expression in osteosarcoma cultured on the surfaces after 7 days. **(D)** *ALP*, *COL1*, *BMP2* and *RUNX2* mRNA expression in osteoblasts cultured on the surfaces after 7 days. **(E)** Immunofluorescence staining of MMP2 and MMP9 in intrascaffold-cultured osteosarcoma cells after 7 days. Scale bar: 50 μm. **(F)** Immunofluorescence staining of ALP and OCN in intrascaffold-cultured osteoblasts after 7 days. Scale bar: 50 μm. **(G)**

Representative blots and fold induction of ITGB, CTNNA1, CTNNB1, FAK and GAPDH in osteosarcoma cells cultured on surfaces after 7 days. **(H)** Representative blots and fold induction of ITGB, CTNNA1, CTNNB1, FAK and GAPDH in osteoblasts cultured on surfaces after 7 days. n=3; mean ± SD; *P<0.05, **P<0.01, ***P<0.001; NS, not significant. L, M and H correspond to low (0.05% GelMA), middle (0.2% GelMA) and high (0.5% GelMA) adhesion ligand density.

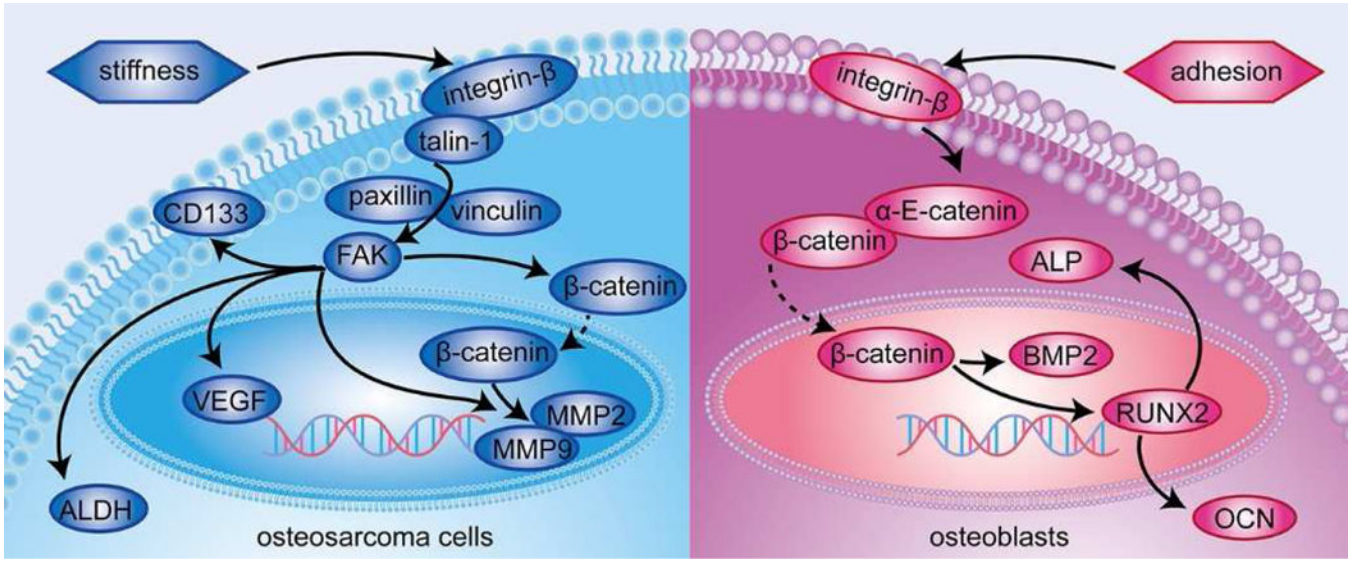

Fig. 9. Mechanism by which osteosarcoma cells and osteoblasts respond to ECM stiffness and adhesion ligands, respectively.

ECM stiffness rather than matrix adhesivity affects osteosarcoma cell growth through regulation of the integrin-mediated FA signaling pathway, whereas osteoblasts are mainly affected by ECM adhesion ligands through modulation of the integrin-mediated AJ signaling pathway.

Table 1.

The theoretical composition of different hydrogels

PEG content / GelMA Content	5%	10%	15%	Adhesivity
0.05%	PEG 25 μL GelMA 25 μL PBS 450 μL initiator 2.5 μL	PEG 50 μL GelMA 25 μL PBS 425 μL initiator 5 μL	PEG 75 μL GelMA 25 μL PBS 400 μL initiator 7.5 μL	**L (Low)**
0.2%	PEG 25 μL GelMA 100 μL PBS 375 μL initiator 2.5 μL	PEG 50 μL GelMA 100 μL PBS 350 μL initiator 5 μL	PEG 75 μL GelMA 100 μL PBS 325 μL initiator 7.5 μL	**M(Middle)**
0.5%	PEG 25 μL GelMA 250 μL PBS 225 μL initiator 2.5 μL	PEG 50 μL GelMA 250 μL PBS 200 μL initiator 5 μL	PEG 75 μL GelMA 250 μL PBS 175 μL initiator 7.5 μL	**H (High)**
Stiffness	**1.6 kPa**	**6 kPa**	**25 kPa**	

Table 2.

The volumes of osteosarcoma cells and osteoblasts with different hydrogels *in vivo*

Stiffness Adhesivity	1.6 kPa	6 kPa	25 kPa	Cell type
L (Low)	123.67±7.1* mm^3	318.30±9.13* mm^3	918.90±5.12* mm^3	osteosarcoma cells
	113.37±7.07# mm^3	110.47±8.57# mm^3	112.63±2.79# mm^3	osteoblasts
M (Middle)	119.40±10.34* mm^3	316.53±7.04* mm^3	917.37±20.54* mm^3	osteosarcoma cells
	314.13±7.46# mm^3	315.47±4.64# mm^3	318.70±7.56# mm^3	osteoblasts
H (High)	119.03±7.26* mm^3	315.60±9.80* mm^3	917.70±12.74* mm^3	osteosarcoma cells
	896.9±1.51# mm^3	901.73±9.57# mm^3	908.17±9.36# mm3	osteoblasts

* indicates $p<0.05$ among samples of different stiffnesses with same adhesivity in osteosarcoma cells

# indicates $p<0.05$ among samples of different adhesivities with same stiffness in osteoblasts